

Morphology of Polypropylene Films Treated in CO₂ Plasma

MOHAMMED AOUINTI,¹ ALAIN GIBAUD,² DANIEL CHATEIGNER,³ FABIENNE PONCIN-EPAILLARD¹

¹Polymères, Colloïdes et Interfaces Unité Mixte de recherche (UMR CNRS 6120), Université du Maine, Avenue Olivier Messiaen, 72085 Le Mans Cedex 09, France

²Physique de l'Etat Condensé (UMR CNRS 6087), Université du Maine, Avenue Olivier Messiaen, 72085 Le Mans Cedex 09, France

³Laboratoire Cristallographie et Sciences des matériaux (CRISMAT) (UMR CNRS 6508), Ecole Nationale Supérieure d'Ingénieurs de Caen, Boulevard Maréchal Juin, 14050, Caen, France

Received 10 July 2003; revised 7 January 2004; accepted 22 January 2004

DOI: 10.1002/polb.20071

Published online in Wiley InterScience (www.interscience.wiley.com).

ABSTRACT: One of the most important claims for the plasma technique as a surface treatment is that it modifies only a few atomic layers of materials. However, with polymers, this assumption must be carefully verified to keep the bulk mechanical properties constant. Besides the oxidation of the film, with specific plasma conditions such as high power and duration, the polypropylene film structure is also modified in the bulk through vacuum ultraviolet absorption and thermal relaxation. This change is associated with smectic- and amorphous-phase transformation into an α -monoclinic phase, with a rapid rate for the smectic transformation and a slower rate for the amorphous transformation. At the same time, the crystallite size increases, and the polypropylene film texture is planar and moderated (1.7 mrd at the maximum of the distribution, with a discharge power of 100 W and a treatment duration of 10 min).

© 2004 Wiley Periodicals, Inc. *J Polym Sci Part B: Polym Phys* 42: 2007–2013, 2004

Keywords: plasma; poly(propylene) (PP); texture; orientation distribution function (ODF); crystallization

INTRODUCTION

The plasma modification of polymer surfaces is a powerful technique in many application fields, such as painting, adhesion, biomaterials, and electronics. This technique may be considered a green and rapid method because no solvent is necessary and only a few minutes are needed. The treatment is considered to be a universal technique because with the same apparatus, hydrophilic or hydrophobic surfaces can be obtained.

One of the most important claims of this technique is that the modification affects only the first few atomic layers of materials. However, with polymers, this assumption must be carefully verified.

In a previous work, the modification of the bulk structure of isotactic polypropylene modified in a nitrogen plasma was reported under specific conditions.¹ These corresponded to so-called drastic conditions, that is, a high discharge power (>80 W) and a long treatment time (>5 min). The initial polymer mostly consisted of smectic and amorphous phases crystallized under irradiation in the so-called α phase. If a thermal effect is not excluded to explain such a transformation, the phenomenon is associated with vacuum ultraviolet

Correspondence to: F. Poncin-Epaillard (E-mail: fabienne.poncin-epaillard@univ-lemans.fr)

Journal of Polymer Science: Part B: Polymer Physics, Vol. 42, 2007–2013 (2004)
© 2004 Wiley Periodicals, Inc.

let (VUV) absorption. When a sample is cooled with a liquid nitrogen system, crystallization still exists but not in such a high proportion. Therefore, the thermal effect affects the material but not predominantly.¹ The emission of short-wavelength radiation, more and more mentioned in the literature as an important agent of polymer chemical modification, depends strongly on the nature of the gas in the following order: H₂ plasma > N₂ plasma > O₂ plasma > He plasma. The nature of the gas directly influences the crystallization kinetics of different polypropylene films treated in such plasmas.¹ O₂ plasma is the most efficient, and helium is the least efficient, in terms of structural modification.

Polypropylene is mostly used as thin films (typically ca. 100 μm thick), such as in the food industry. Because the crystallized phases of polypropylene are of low symmetry, their mechanical behavior will be different when they are amorphous or crystallized. Furthermore, in the crystallized form(s), the stabilization of a texture may considerably influence the mechanical responses, giving anisotropic macroscopic deformations and stresses in the materials, which backward could be of importance for their optimized use. It becomes then of major importance to examine how crystal phases develop under plasma irradiation in thin films of polypropylene and if eventually this crystallization is accompanied by a texture development.

In this work, we concentrate on the characterization of CO₂-plasma-treated films of polypropylene. The amounts, structures, and crystallite sizes of the crystalline phases grown under irradiation are characterized with X-ray diffraction. The preferred orientation of the crystallites are quantitatively determined with X-ray diffraction peak analysis.

EXPERIMENTAL

Polypropylene

The polypropylene, supplied by Institut Textile de France, was an isotactic, semicrystalline polymer synthesized with a Ziegler–Natta catalyst (melting point = 160 °C, as determined by differential scanning calorimetry). The concentration of the initial crystalline phase was estimated to be roughly 38 vol %, and this phase corresponded to the smectic state.

Before the plasma treatment, 100-μm-thick films were successively washed with ethanol and acetone and then dried *in vacuo* for 1 day.

Plasma Treatment

The equipment was a microwave plasma apparatus. The plasma excitation was provided by a Sairem 433-MHz variable-power (0–250 W) microwave generator, which was coupled to a resonant cavity. The incident power and the reflected power (P_r) were measured with a Hewlett–Packard 435B power meter. The impedance was adjusted until P_r was low ($P_r < 0.02$ W). The glow was generated at the top of the reactor. The pumping system was composed of primary (CIT Alcatel 2012) and oil-diffusion (CIT Alcatel Crystal) pumps. An MKS 1259B mass-flow meter controlled the gas flow [F (sccm)]; grade N45 CO₂ was purchased from Air Liquide (purity > 99.995%). The pressure [p (mbar)] was measured with Penning and Pirani gauges. The reactor was a quartz cylinder 500 mm long and 76 mm in diameter. The reactor was set up in a chamber used for the sample introduction. The substrate could be moved into or out of the plasma area. d (cm) represents the distance between the bottom of the excitatory source and the sample

The parameters of the plasma treatment were as follows: $F_{\text{CO}_2} = 20$ sccm, $p = 7.5 \times 10^{-1}$ mbar, $d = 4$ cm, $t = 10$ min [when the power (P) was varied from 0 to 100 W], and $P = 100$ W (when t was varied from 0 to 11 min).

X-Ray Scattering and Texture Analysis

The X-ray structure and crystallite size characterization was run on a Philips X'PERT diffractometer in the Bragg–Brentano mode. A silicon standard was used to define the instrumental resolution, and Rietveld refinement was performed with the help of the Rietquan program.² X-ray quantitative texture analysis was measured on a Huber four-circle diffractometer equipped with a CPS 120 curved position-sensitive detector from INEL, as detailed elsewhere.³ The use of such a detector is essential for polypropylene films because broad diffraction peaks strongly overlap. Using a classical four-circle diffractometer equipped with a point detector, one fixes the Bragg angle (θ) of the diffractometer before scanning individually each necessary pole figure with two other angles (χ and ϕ) that conserve θ . Un-

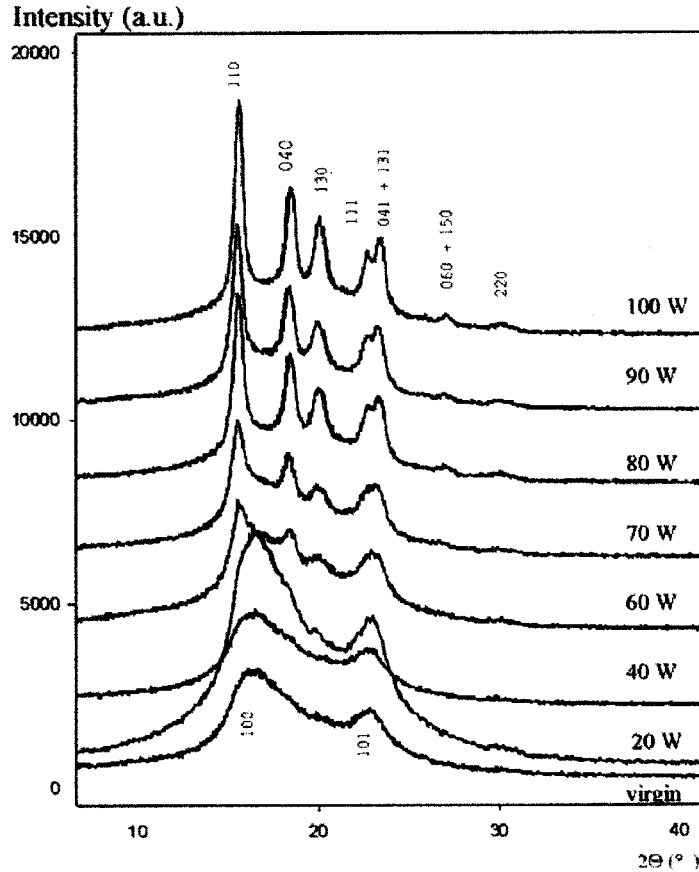


Figure 1. X-ray diffraction diagrams of plasma-treated polypropylene films versus the discharge power ($F_{\text{CO}_2} = 20$ sccm, $p = 7.5 \times 10^{-1}$ mbar, $d = 4$ cm, $t = 10$ min).

fortunately, for strongly overlapped peaks, at one θ position, several peak contributions correspond in unknown relative amounts, and this precludes any quantitative analysis. With a CPS, all the peak profiles are measured for all sample positions in a reasonable experimental time, which allows the separation of each peak contribution. In the first approach, regular ϕ scans corresponding to a rotation of the sample about its surface normal showed that the texture was symmetric around the normal to the film plane. Then, we measured χ scans (by rotating the sample about an axis contained within the plane of the film) with 5° steps and at a counting time of 1800 s per χ position at an incidence angle of $\omega = 10^\circ$, which corresponded approximately to the Bragg position of the {111,041,131} triplet. The films were large enough to ensure that the X-ray beam was fully intersecting the sample up to $\chi = 65^\circ$. The amorphous part was removed under the assumption of a linear variation under each of the peaks. Data reduction (volume/absorption and localization

corrections) was performed with our program Pofint,⁴ whereas the orientation distribution (OD) refinement was operated on the extracted pole figure data with the Williams-Imhof-Matthies-Vinel (WIMV) direct method, as implemented in the Beartex package.⁵ The OD is a three-dimensional mathematical object that represents how the orientations of the crystallites are distributed in a specific sample. Indeed, one cannot directly compare diffracted intensities to evaluate the crystallite orientations from sample to sample because these intensities also depend strongly on the porosity, crystalline state, strains, phase ratio, and so forth. The OD allows the normalization of the diffraction measurements in such a way that only the orientation is of concern.⁶ The results are then expressed in orientation densities [multiples of a random distribution (mrd)]. A perfectly randomly oriented sample (powder) will exhibit all its pole figures with homogeneous 1 mrd density levels, whereas a textured sample will show pole figures with density maxima in the pole

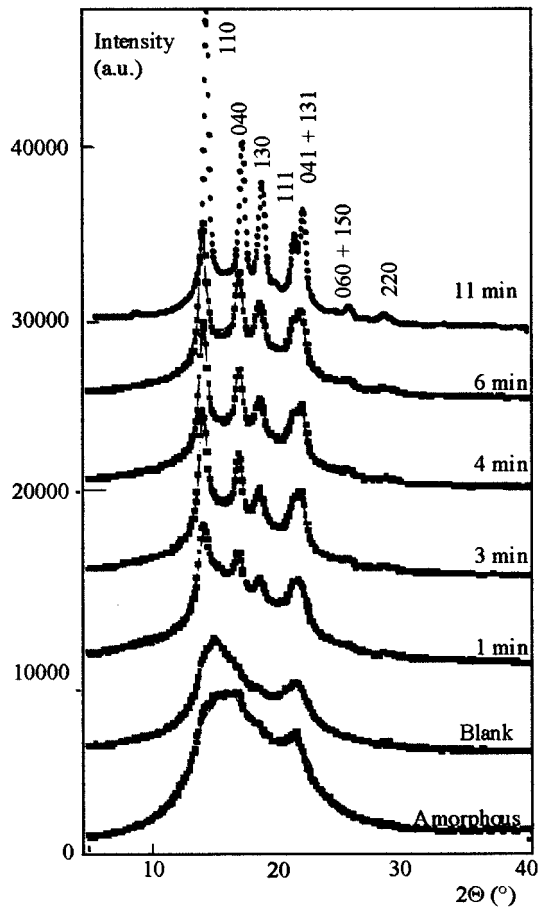


Figure 2. X-ray diffraction diagrams of plasma-treated polypropylene films versus the treatment duration ($F_{\text{CO}_2} = 20$ sccm, $p = 7.5 \times 10^{-1}$ mbar, $d = 4$ cm, $P = 100$ W): (—) experimental data and (---) calculated data.

figures for the directions of texture and minima elsewhere.

RESULTS

The crystallinity (amorphous-to-crystalline ratio), crystallite sizes, cell parameters, and texture

Table 1. Different Sets of Calculated Parameters of Monoclinic Units

a	b	c	γ	Reference
6.66	6.50	20.86	98.68	This work
6.63	6.50	20.78	99.50	14
6.63	6.52	20.98	98.50	15
6.66	6.50	20.78	99.62	16
6.65	6.50	20.78	99.60	17
6.65	6.50	20.96	99.33	18

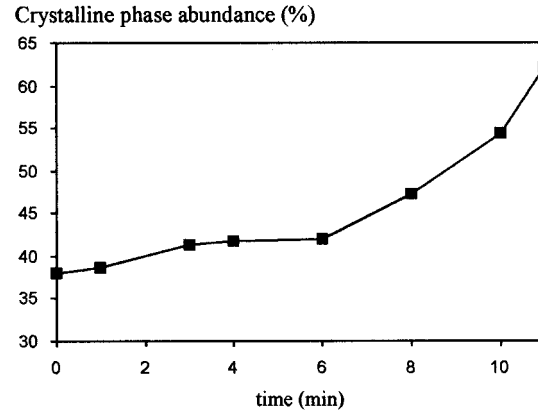


Figure 3. Crystalline-phase abundance of plasma-treated polypropylene films versus the duration.

of isotactic polypropylene treated under specific conditions of CO_2 plasma, as described in ref. 7, have been analyzed.

Structural and Microstructural Evolution

The observed crystallographic structures of virgin and treated polypropylene correspond to the smectic⁸⁻¹² and monoclinic (α)^{12,13} phases, respectively (Figs. 1 and 2).

The virgin sample pattern exhibits two principal reflections, (100) and (101), at 2θ values of 15 and 21°, respectively. These reflections are associated with the smectic phase of isotactic polypropylene.^{14,15} A third broad reflection ($2\theta = 17^\circ$) is identified as the amorphous phase.¹⁵

We neatly observe a phase transition from the smectic phase to the monoclinic phase beginning

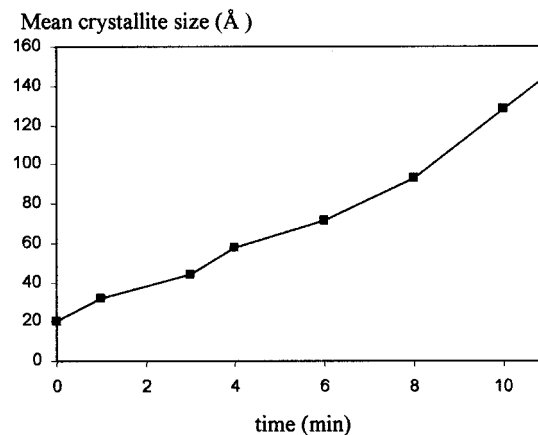


Figure 4. Mean crystallite sizes of plasma-treated polypropylene films versus the duration.

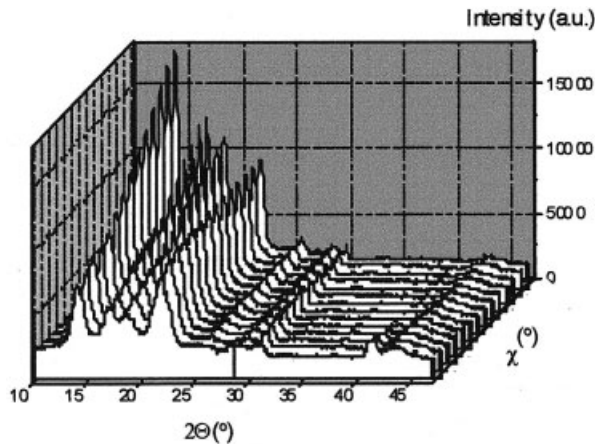


Figure 5. X-ray diffraction diagrams of 11-min-plasma-treated films measured as a function of the tilt angle χ ($\chi = 0$ in the back plane, $\chi = 65^\circ$ in front, χ step = 5°).

after 1 min of treatment. After 11 min, the transformation is fully achieved at this plasma power. As a result of the increase in crystallization with irradiation, the peak intensities increase with time. Furthermore, their full width at half-maximum decreases, and this indicates an overall growth of the crystallite sizes.

The Rietveld refinements of the diagrams indicate crystallographic structures very close to the ones already given in the literature.^{16–20} We obtain for the most crystallized film the following: $a = 6.66 \text{ \AA}$, $b = 6.5 \text{ \AA}$, $c = 20.86 \text{ \AA}$, and $\gamma = 98.7 \text{ \AA}$ (Table 1).

The crystalline-phase abundance was obtained through the refinement of the structure under the assumption of the coexistence of an amorphous phase and a crystalline phase in the films. A reference amorphous sample (see Fig. 2) was used to define the scattering profile of the amorphous phase. The amount of each phase was determined through the refinement of the scale factor of each phase. During this procedure, the amorphous-phase scattering profile was fixed to that of the reference sample, and only the scale factor was allowed to vary. The lattice parameters, the scale factor, and the broadening of the Bragg peaks of the crystalline phase were refined. The amount of the crystalline phase increases slowly for a short duration, to less than 5% up to 6 min of treatment (Fig. 3); it then increases rapidly, reaching more than 63% at 11 min of treatment. The crystallite sizes are directly obtained from the refinement of the width of the Bragg peaks. Each peak profile results from the convolution of instrumental and

sample signals, the former being calibrated on a perfectly crystallized sample. The sample contribution is divided in two parts, one coming from the finite size of the crystallites giving a Lorentzian contribution, the other from microstrains contributing with a Gaussian shape. No significant microstrain could be detected in our samples (for more details, see ref. 2). The mean crystallite sizes of our samples (Fig. 4) varied similarly to their crystalline ratio, reaching approximately 150 Å at 11 min of treatment. Crystallinity nucleation is then accompanied by crystal growth.

Quantitative Texture Analysis

Looking at the evolution of diffraction lines with the tilt orientation angle χ (Fig. 5), we can see that the intensities of the reflections $\{110/011\}$, $\{040\}$, and $\{-111/130/031\}$ decrease with χ , whereas the $\{111/-131/041/121\}$ group remains almost constant (because of defocusing, its maximum decreases and its integrated value increases).

We used all four indicated groups and the refined values of the cell parameters to refine the OD of the crystallites. To determine the OD with a satisfying degree of confidence, we have to define each OD cell by at least three independent measurements. In our case, the measured pole figures define the OD with 3–17 independent measurements (Fig. 6). These values may be enhanced with weaker diffraction lines, but with our counting times, reflections at larger 2θ values were much too noisy.

The first measured pole figures and the second ones recalculated from the refined OD compare favorably (Fig. 7); reliability factors²¹ were averaged on all the pole figures for all the density levels ($RP_{0.05}$) and for the densities above 1 mrd

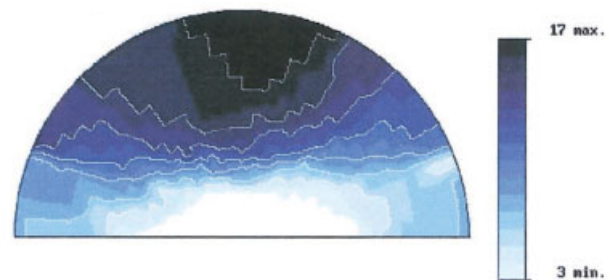


Figure 6. Linear-scale, equal-area projection showing the number of independent measurements per OD cell (MIMA subroutine of the Beartex program).

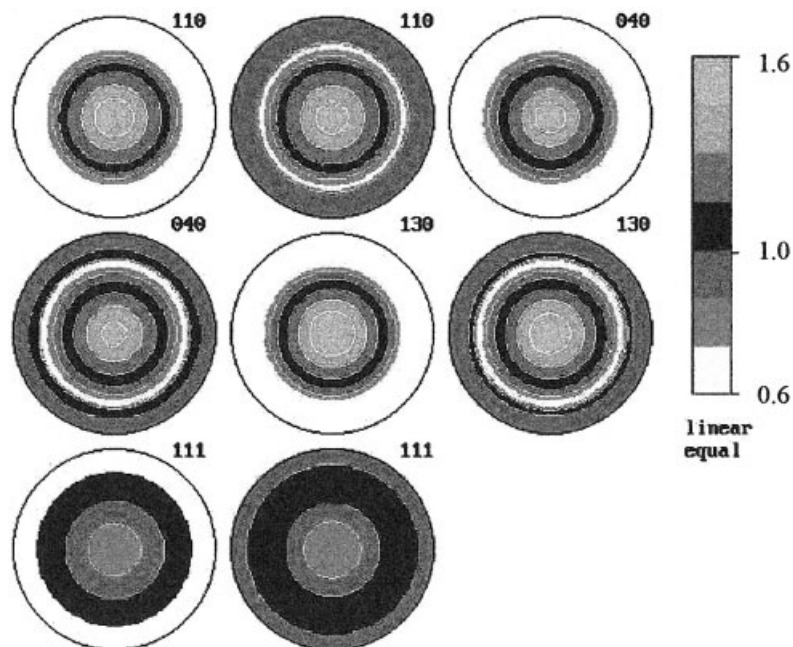


Figure 7. Experimental and recalculated normalized multipole figures, which reveal the quality of the refinement. Linear-density-scale, equal-area projection (mrd).

(RP_1) to be as low as 1.4 and 1%, respectively. The texture strength is relatively low, with a texture index of 1.35 mrd².²² The orientation corresponds to the alignment of c axes randomly in the plane of the film, with a random orientation of the a and b axes around c , as denoted by the recalculated low Miller index pole figures (Fig. 8). This orientation type corresponds to a planar texture with only 1° of rotation freedom for the crystallites.

DISCUSSION

The structural transformation observed under plasma irradiation appears to be a parallel occurrence of two different phenomena. In the first minute of irradiation, the complete crystallization of the smectic phase is achieved in the initial films and is transformed into the α -polypropylene phase. An additional slow crystallization and growth process of the α phase takes place at the expense of the amorphous phase. The transformation appears as a continuous process, with a progressive chain organization, the incidences of which are the texture formation with the longest axis in the plane of the film. This implies lateral motions; macromolecular chains turn over to set up the helices of the α phase in the observed orientation, as previously thought.¹⁵

The alteration, initiated by the plasma energy source, may be promoted either by a direct energy-transfer bombardment from ions (in the 0–100-eV range) and metastable species (0–20 eV) on a thickness scale of 10–20 Å or by indirect radiative absorption, particularly visible or ultra-

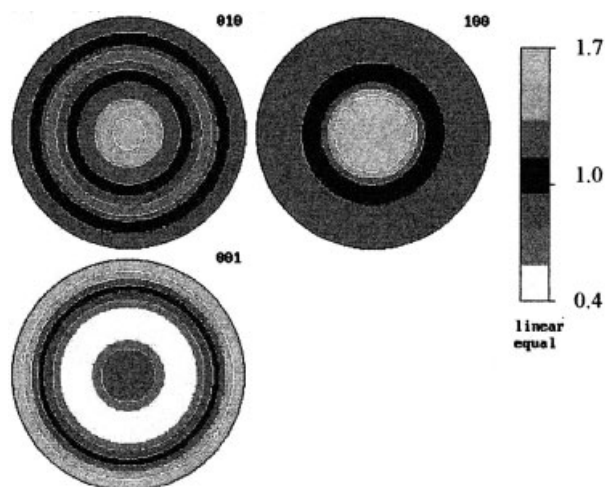


Figure 8. Linear-density-scale, equal-area projection (mrd) showing recalculated {010}, {100}, and {001} normalized pole figures, which reveal the alignment of the c axes of α -polypropylene in the film plane (planar texture).

violet photons, the action of which is known to be effective on a thickness scale greater than 10 μm in this kind of material. The latter is probably responsible for such a transformation, by analogy to previous works on polypropylene treatment under nitrogen plasma,¹ which could also apply to the CO₂ treatment. However, if the thermal relaxation resulting from a too low excitation energy is not enough to break polymer bonds efficiently, the corresponding energy may be used for local chain rearrangements and promotion of the texture.⁹

CONCLUSIONS

Besides the superficial modification of polypropylene films, the structural and microstructural modifications of 100- μm -thick polypropylene films by specific CO₂ plasma conditions (high power and long treatment times) have been characterized with X-ray diffraction. The polypropylene film structure is modified in the bulk mostly through VUV absorption and thermal relaxation. This structural change is associated with a phase transition from the smectic and amorphous phases into the α -monoclinic phase, with rapid and then slower kinetics for the first transformation and a slower rate for the latter one. During both transformations, the mean crystallite size increases, and the stabilization of a planar texture is achieved in the film. The texture strength is moderate, with the longest cell parameter at random in the plane of the film, for the more drastically treated film.

REFERENCES AND NOTES

1. Poncin-Epaillard, F.; Brosse, J. C.; Falher, T. *Macromolecules* 1997, 30, 4415.
2. Lutterotti, L.; Scardi, P.; Maistrelli, P. *J Appl Crystallogr* 1992, 25, 459–462.
3. Ricote, J. J.; Chateigner, D. *Bol Soc Española Cerám Vidrio* 1999, 38, 587.
4. Chateigner, D. POFINT: Pole Figure Interpretation; Centre National de la Recherche Scientifique-INEL SA (Artenay F 45410, licence n° L03048): 2002.
5. Wenk, H. R.; Matthies, S.; Donovan, J.; Chateigner, D. *J Appl Crystallogr* 1998, 31, 262.
6. Wenk, H.-R. In *An Introduction to Modern Texture Analysis*; Wenk, H. R., Ed.; Academic: New York, 1985.
7. Aouinti, M.; Bertrand, P.; Poncin-Epaillard, F. *Plasma Polym* 2003, 8, 225–236.
8. Natta, G. *Makromol Chem* 1960, 35, 94.
9. Gailey, J. A.; Ralston, R. H. *Soc Plast Eng Trans* 1964, 4, 29.
10. Miller, R. L.; *Polymer* 1960, 1, 135.
11. Gezovich, D. M.; Geil, P. H. *Polym Eng Sci* 1968, 8, 202.
12. Border, G.; Grell, M.; Kallo, A. *Faserforsch Text-Tec* 1964, 15, 527.
13. Kawamoto, N.; Mori, H.; Nitta, K. H.; Sasaki, S.; Yui, N.; Terano, M. *Macromol Chem Phys* 1998, 199, 261.
14. Tanaka, H. *Eur Polym J* 1991, 27, 565.
15. Mc Allister, P. B.; Carter, T. J.; Hinde, R. M. *J Polym Sci Polym Phys Ed* 1978, 16, 49.
16. Mencik, Z. *J Macromol Sci Phys* 1972, 6, 101.
17. Ferro, D. R.; Bruckner, S.; Meille, S. V.; Ragazzi, M. *Macromolecules* 1992, 25, 5231.
18. Turner-Jones, A.; Airzlewood, J. M.; Becket, D. R. *Macromolecules* 1964, 75, 134.
19. Stocker, W.; Magonov, S. N. B.; Wittmann, H. J. C.; Lotz, B. *Macromolecules* 1993, 26, 5915.
20. Nishimoto, S.; Kagiya, T. In *Handbook of Polymer Degradation*; Hamid, S.; Amin, M. B.; Maadhad, A. G., Eds.; Marcel Dekker: New York, 1992; p 3.
21. Matthies, S.; Vinel, G. W.; Helming, K. *Standard Distributions in Texture Analysis*; Akademie-Verlag: Berlin, 1987.
22. Bunge, H. J. *Texture Analysis in Materials Science*; Morris, P. R., Translator; Butterworths: London, 1982.